Title

Pyrazine-Fused Porous Graphitic Framework-Based Mixed Matrix Membranes for Enhanced Gas Separations

Journal

ACS Applied Materials & Interfaces, 12(14)

ISSN

1944-8244

Authors

Ma, Canghai

Li, Xinle

Zhang, Jian

et al.

Publication Date

2020-04-08

DOI

10.1021/acsami.0c01378

Peer reviewed

Pyrazine-fused Porous Graphitic Frameworks-based mixed matrix membranes for enhanced gas separations

Canghai Ma‡, Xinle Li‡, Jian Zhang*, Yi Liu*, and Jeffrey J. Urban*

The Molecular Foundry, Lawrence Berkeley National Laboratory, 1 Cyclotron Rd, Berkeley, CA 94720, USA

KEYWORDS: Porous graphitic frameworks, mixed-matrix membranes, separation, CO_2 capture, hydrogen regeneration

ABSTRACT: Membrane-based separations can mitigate the capital- and energy-intensive challenges associated with traditional thermally driven processes. To further push the boundary of gas separations, mixed matrix membranes (MMMs) have been extensively exploited; however, identifying an optimal nanofiller to boost the separation performance of MMMs beyond Robeson permeability-selectivity upper bounds remains an ongoing challenge. Here, a new class of MMMs based on pyrazine-fused crystalline Porous Graphitic Frameworks (PGFs) is reported. At a loading of 6 wt% PGFs, the MMMs surpass the current H_2/CH_4 Robeson upper bound, ideally suited for applications such as H_2 regeneration. In addition, the fabricated MMMs exhibit appealing CO_2 separation performance, approaching closely current Robeson upper bounds for CO_2 separation. Compared with the pristine polymeric membranes, the PGFs-based MMMs display a record-high enhancement of gas permeability over 120% while maintaining intrinsic gas selectivities. Highlighting the crucial role of the crystallinity of nanofillers, this study demonstrates a facile and effective approach in formulating high-performance MMMs, complementing state-of-the-art membrane formation processes. The design principles open the door to energy-efficient separations of gas mixtures with enhanced productivity compatible with the current membrane manufacturing.

1. INTRODUCTION

A gas separation membrane serves as a barrier that selectively passes through one gas molecule over another, which has exhibited enormous potential in reducing the capital cost and energy consumption associated with conventional thermally-driven industrial gas separation processes (e.g. distillation) [1]. In the realm of seeking next-generation membrane materials to meet the increasing demands for high recovery and purity in separating gas mixtures, growing attention has been shifted towards inorganic materials such as zeolites, metal-organic frameworks, and carbon molecular sieves [2]. In this category, atomically thick two-dimensional (2D) graphene-based materials have emerged as an advanced molecularly selective material for separating gas mixtures, attributed to its minimal transport resistance and tailorable pore aperture for discriminating gas molecules with similar sizes [3-6]. Graphene-based membranes have demonstrated extraordinary separation performance for several gas pairs, such as O_2/N_2[7], CO_2/N_2[7-8], H_2/CO_2[9], H_2/N_2[10]. A chemically-synthesized class of graphene derivative, pyrazine-fused porous graphitic frameworks (PGFs), featuring fully annulated aromatic skeletons with periodic pores linked via pyrazine rings, have displayed enormous potential in a plethora of areas including supercapacitors [11], catalysis [12-13] and desalination [14]. Despite the promise, there is limited chemical functionality available with PGFs. For this reason, to our knowledge, the use of pyrazine-fused PGFs as a gas separation membrane material remains unexplored.

Prior attempts to synthesize 2D PGFs led to predominantly amorphous crosslinked polymers, leaving crystalline PGFs with clear structural integrity an elusive target [11]. In a recent effort to overcome this challenge, we developed a unique dynamic synthesis under basic aqueous conditions to afford a crystalline PGF (termed as PGF-1), which displayed extraordinary performance as an organic cathode for lithium-ion batteries[15]. In recognizing the nanoporous 2D feature and the high nitrogen-content of this crystalline PGF, we aim to explore its potential as a high-performance nanofiller for fabricating gas separation membranes. In analogy to inorganic membranes such as zeolites [16] and metal-organic frameworks [17], PGFs are readily made into composite membranes on porous support or free-standing neat membranes without support, which, however, face challenges of skin integrity when scaling-up [2, 16, 18-19]. An appealing approach to mitigate this hurdle is to utilize a mixed matrix membrane (MMM) technology. MMMs are fabricated by mixing a nanofiller (i.e. disperse phase) with polymers (i.e. continuous phase) to create an organic/inorganic hybrid structure. MMMs simultaneously integrate advantages of

each component in the membranes, i.e., easy processing of polymers and molecular sieving of nanofillers [20-23], thereby enhancing the gas separation performance [23]. In addition, the MMM technology is highly scalable since the nanofillers are readily mixable with the polymers in the manufacturing process of membranes (e.g. hollow fiber membranes) [24]. Despite those advantages, a vast majority of reported MMMs generally perform below the Robeson upper bounds, i.e., tradeoffs of gas permeability and selectivity [22-23, 25], constraining their practical application in gas separations.

To tackle this challenge, we report a facile and effective route to developing pyrazine-fused PGFs-based MMMs by incorporating PGF-1 into a polyimide polymer, 6FDA-DAM: DABA (3:2) (6FDD) (denoted as PGF-1-6FDD MMMs). The obtained MMMs exhibit unparalleled gas separation performance in comparison with the reported membranes. At only 6 wt% PGF-1 loading, the MMMs exhibit a H_2/CH_4 separation efficiency crossing the current Robeson H_2/CH_4 upper bound and closely approach the current Robeson upper bounds for multiple gas pairs, including CO_2/CH_4, CO_2/N_2, and H_2/N_2. We further compared PGF-1 with its amorphous analog, AP-1 to investigate the effect of crystallinity on gas separation. Results show that the crystalline PGF-1 leads to a more pronounced permeability enhancement to MMMs than their amorphous analog (termed as AP-1), highlighting the critical role of crystallinity in achieving enhanced separation efficiency. To our knowledge, this work represents the first report of using pyrazine-fused PGFs to significantly improve gas separation performance of MMMs, which may find broad applications in CO_2 capture, natural gas separation, and hydrogen regeneration.

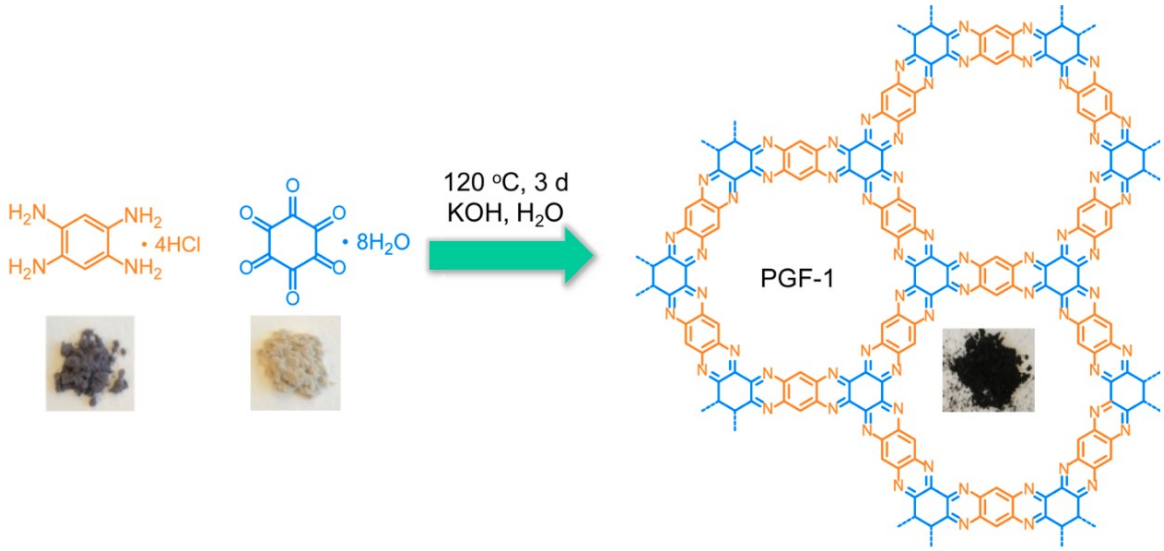

Figure 1: Dynamic synthesis of crystalline PGF-1 under basic aqueous conditions. Hexaketocyclohexane octahydrate reacts with 1,2,4,5-benzenetetramine tetrahydrochloride in aqueous solutions using potassium hydroxide (4 M) as the catalyst.

2. EXPERIMENTAL SECTION

Synthesis of PGF-1.As described in Figure 1, a 5 mL Microwave Biotage vial was charged with 1,2,4,5-benzenetetramine tetrahydrochloride (25.6 mg, 0.045 mmol), hexaketocyclohexane octahydrate (18.6 mg, 0.06 mmol) and deionized water (2 mL) and sonicated for 30 min to form a slurry suspension. A potassium hydroxide solution (4 M, 0.2 mL) was then added into the mixture and sonicated for 10 min, and degassed by three cycles of freeze-pump-thaw under vacuum, followed by heating at 120 °C for 3 d. Afterward, the black precipitate in the mixture was filtered and washed with water and methanol, followed by drying under vacuum at 120 °C for 1 d.

Synthesis of amorphous AP-1.The AP-1 was synthesized following the procedures described in reference with slight modifications [12]. A 5 mL Microwave Biotage vial, charged with 1,2,4,5-benzenetetramine tetrahydrochloride (50 mg, 0.176 mmol) and hexaketocyclohexane octahydrate (36.5 mg, 0.118 mmol) in a nitrogen atmosphere, was placed in an ice bath, followed by adding 4 mL deoxygenated NMP with 0.025 mL of sulfuric acid (98%). After warming up to room temperature in 2 h, the reaction mixture was sealed in nitrogen and heated at 180 °C for 16 h. Afterward, the mixture was allowed to cool down to room temperature and the black solid was collected by filtration and Soxhlet extracted with water, methanol, and Tetrahydrofuran (THF) for 3 d,

followed by drying under vacuum at 120 °C for 1 d.

Preparation of MMMs. The 6FDD polyimide was synthesized using reported procedures in the literature [26] and dried at 100 °C under vacuum overnight. The polymer was dissolved in tetrahydrofuran (THF) to prepare a 5-10 wt% solution. To make MMMs, a designated amount of nanofillers (PGF-1 or AP-1) was suspended in THF by sonication, and the suspension was primed by adding ~10% of the above-mentioned polymer solution, followed by adding the remaining polymer solution. Excessive THF in the suspension was removed by nitrogen purging to achieve a polymer concentration of 5-10 wt% in mixture. The solution was cast onto a plate to form MMMs. Membranes were dried at 200 °C for 1 h under vacuum to remove any residual solvents.

Permeation and characterizations of membranes. The membrane sample was tested with a house-made constant volume/variable pressure permeation setup. Prior to gas permeation, the entire system was pulling vacuum thorough and the leak rate of the system was less than 1% of gas permeation rate for each test. The pure gas was introduced into the membrane in the order of N_2, CH_4, H_2, and CO_2. Gas permeation was tested at 35 °C with an upstream feeding pressure of 3-17 bar. More details about calculating permeability and selectivity can be found in Supporting Information. Membranes were characterized using TGA, FTIR, and SEM, with procedures described elsewhere [26].

3. RESULTS AND DISCUSSION

3.1. Membrane material characterizations. PGF-1 was synthesized in the laboratory as shown in Figure 1 [15]. Briefly, two porous graphitic materials, i.e. crystalline PGF-1 and its amorphous counterpart (AP-1), were prepared using basic and acidic conditions, respectively. Fundamental physiochemical properties have been characterized previously to gain insights into the PGF-1 structure [15]. Specifically, PGF-1 shows a BET surface area of 101 m^2 g^{-1} and an estimated pore aperture of 1.2 nm as described in our earlier work[15]. Crystalline PGF-1 possesses an internal pore aperture of ~12 Å, which is larger than the majority of gas molecules, thus potentially affording drastically enhanced gas permeability. The powder X-ray diffraction (PXRD) pattern of PGF-1 exhibits strong peaks at 6.1° and 26.4 °, which are assignable to the (100) and (001) planes [15]. Such features match well with the simulated PXRD pattern in an eclipse stacking mode (Supporting Information Figure S1). Thermogravimetric analysis (TGA) indicates their appealing thermal stability against temperature as high as 350 °C (Supporting Information Figure S2). Fourier-transform infrared spectroscopy (FTIR) reveals the characteristic stretching band of C=N in aromatic rings at 1243 cm^{-1} (Supporting Information Figure S3). Scanning Electron Microscope (SEM) images show the nanoflakes morphologies of PGF-1, despite a noticeable aggregation of particles (Supporting Information Figure S4). Overall, these physiochemical characterizations such as the nano-sized structures and

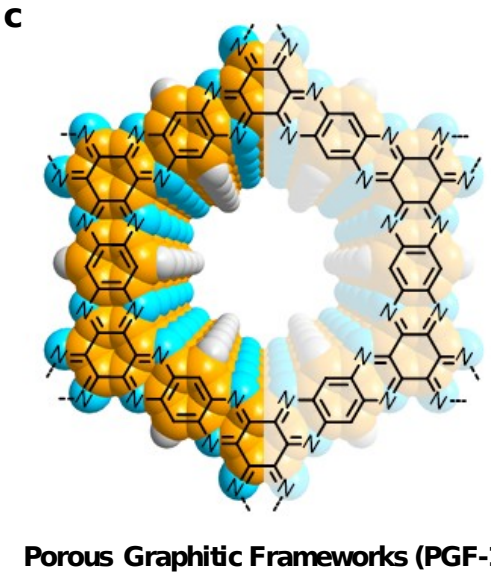

Figure 2. Fabrication of PGF-1-polymer MMMs. (a) Illustrative schematic showing the principle of fabricating MMMs by incorporating PGF-1 into 6FDD polymer; (b) the chemical structure of 6FDD polymer; (c) Space-filling model of crystalline PGF-1 with layers arranged in an eclipsed stacking mode. Color code: C, orange; N, blue; H, gray.

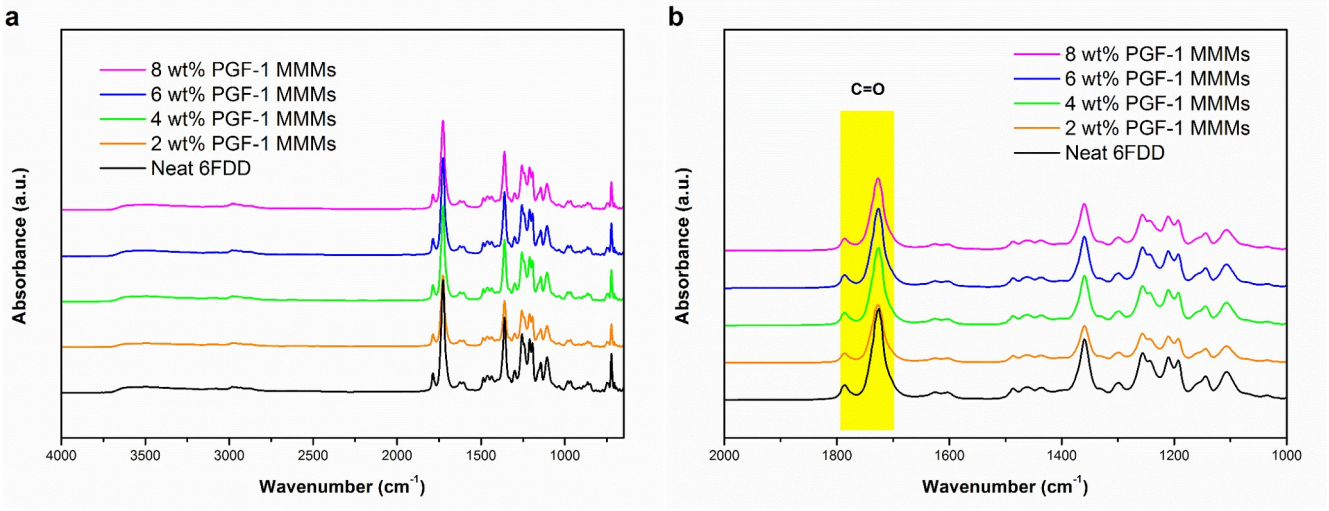

Figure 3: FTIR spectrum of neat 6FDD polymer and PGF-1-6FDD MMMs with various PGF-1 loadings.(a) wavenumber range of 600-4000cm^{-1} and (b) wavenumber range of 1000-2000cm^{-1}. Stretching bands at 1726 cm^{-1} and 1786 cm^{-1} correspond to the asymmetric and symmetric stretching of C=O of the polyimide in MMMs, respectively.

robustness against elevated temperatures confirms the suitability of PGF-1 as an excellent nanofiller to formulate MMMs.

3.2. Membrane characterizations. To prepare MMMs, PGF-1 was blended with a high-performance polyimide, so-called 6FDA-DAM:DABA (3:2) (6FDD) (6FDA = 4,4'-(hexafluoroisopropylidene)diphthalic anhydride; DAM = 2,4,6- trimethyl-1,3-diaminobenzene; DABA=3,5-diamino benzoic acid) with various PGF-1 loadings in the matrices (Figure 2). TGA of MMMs (Supporting Information Figure S5) clearly suggests the strong resilience of membranes against high temperatures. Our membranes withstand temperature as high as 400 °C without decomposition. As expected, MMMs display strong stretching bands at 1726 cm^{-1} and 1786 cm^{-1} in the FTIR spectra (Figure 3), corresponding to the asymmetric and symmetric stretching of C=O in the polyimide, respectively.

In order to obtain smooth cross-sections for SEM study, membrane samples were cryogenically fractured in the presence of liquid nitrogen. SEM results verify the morphologic integrity of membranes, which manifest the excellent interfacial compatibility of PGF-1 and 6FDD polymer without any visible macro-void defects, or so-called "sieve-in-cage" morphology (Figure 4). In addition, PGF-1 is ideally dispersed in the polymer matrix, which in combination with the closely adhered PGF-1/polymer interface lays a solid foundation for the fabrication of defect-free MMMs for gas separations.

3.3. Membrane separation performance. The intrinsic gas transport properties of PGF-1-6FDD MMMs were examined using a constant volume/variable pressure permeation apparatus. Details of calculating gas permeability and selectivity were described in Supporting Information. As illustrated in Figure 5 and Figures S6-S8 in Supporting Information, the introduction of PGF-1 increases both CO_2 and H_2

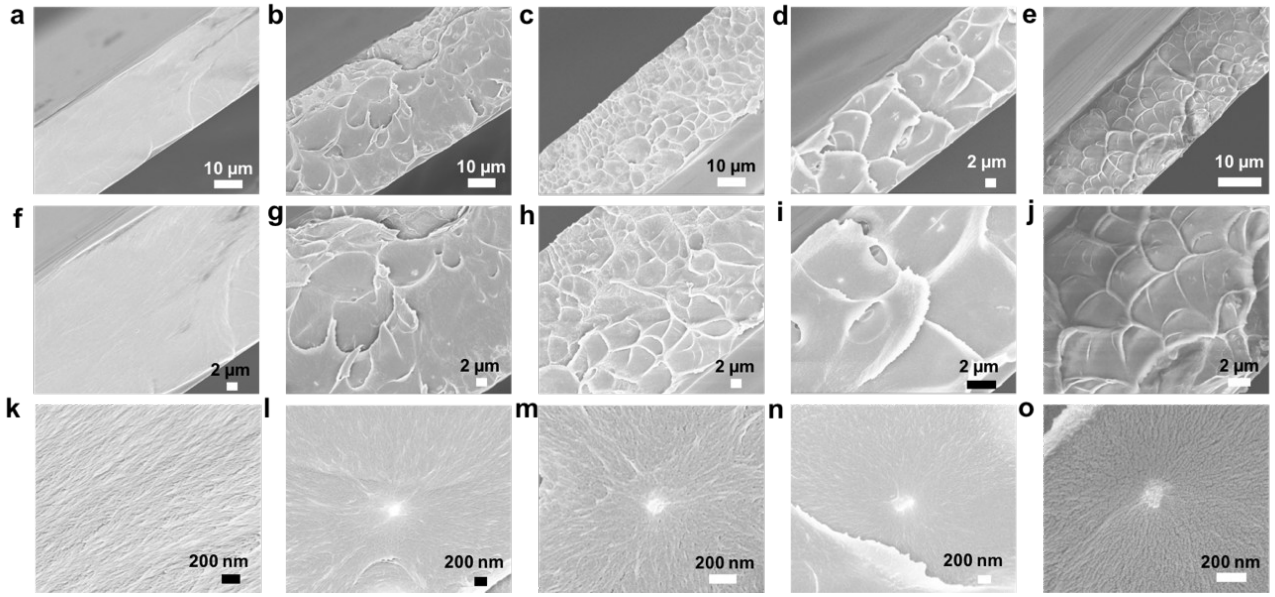

Figure 4. Cross-sectional morphology of PGF-1-6FDD MMMs. Scanning electron microscope images of PGF-1-6FDD MMMs (a) neat polymer (b), 2 wt% (c), 4wt % (d), 6 wt % (e), 8 wt% PGF-1 loading in MMMs. (f)-(j) and (k)-(o) refer to the higher magnifications of the images of (a)-(e), respectively.

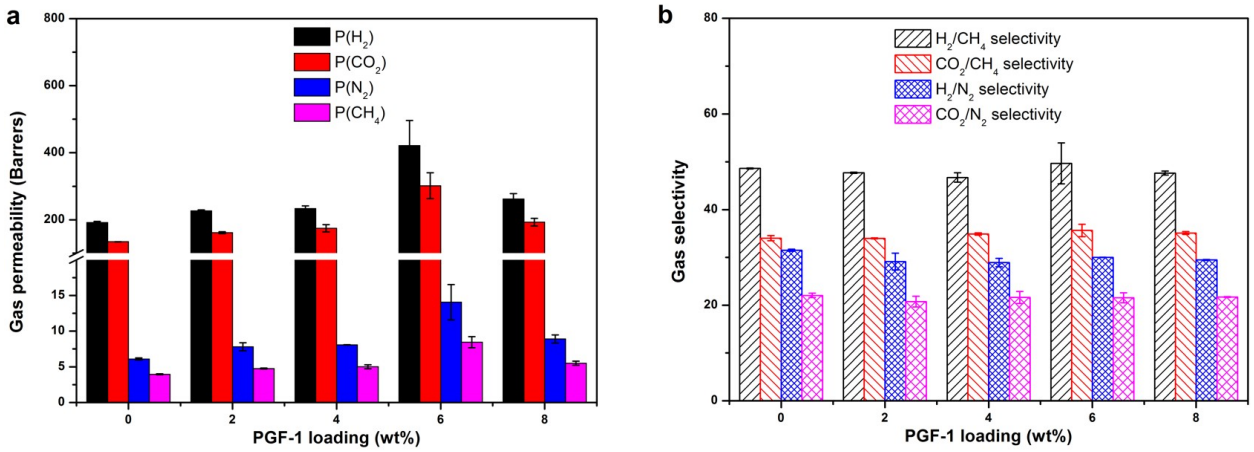

Figure 5. Effects of PGF-1 on PGF-1-6FDD MMMs.(a) gas permeability and (b) gas selectivity of MMMs with various PGF-1 loading. Membranes were tested at 35 ºC, 3 bar.

permeabilities noticeably and an intrinsic gas permselectivity is attained in the span of all loadings. In the presence of 6 wt% PGF-1, the MMMs demonstrate a CO_2 and H_2 permeability of 302 and 421 Barrers, respectively, increasing sharply from 134 and 192 Barrers in the case of pristine polymeric membranes. The CO_2 and H_2 permeabilities are enhanced by over ~120% without losing permselectivities, indicative of an intrinsically defect-free nature of the membranes. The gas permeability increases with PGF-1 loading up to 6 wt% due to the additional free volume of MMMs induced by PGF-1 particles. When further increasing the loading to 8 wt%, the MMMs exhibit a decrease of permeability, similar to trends reported in literatures [27-29]. We suspect that the drop in permeability is likely due to partial pore blockage and polymer chain rigidification[30]. Indeed, the membranes exhibit attractively high gas selectivities with a H_2/CH_4, H_2/N_2, CO_2/CH_4 and CO_2/N_2 selectivity of 49.7, 30.0, 35.6, and 21.6 respectively, with minimal changes as compared with the pristine polymer. It is expected that PGF-1 has negligible effects on enhancing gas selectivity since PGF-1 possesses a pore aperture of 12 Å larger than the size of gas molecules tested in this work. To our delight, imbedding of 6 wt% PGF-1 yields the performance of MMMs above the current Robeson H_2/CH_4 upper bound (Figure 6). Moreover, these membranes exhibit performance beyond prior Robeson upper bounds (1991) and approach current Robeson upper bounds (2008) [25] closely for H_2/N_2 and CO_2/CH_4 separations. Meanwhile, they show decent CO_2/N_2 separation performance, providing an attractive alternative for applications such as CO_2 capture and biogas upgrading. The CO_2 separation performance is

approaching the 2019 upper bounds (CO_2/CH_4 and CO_2/N_2), defined by the benzotriptycene-based polymers of intrinsic microporosity[31]. As shown in Figure S9 in Supporting Information, the membranes also display potential for separating other gas pairs, such as H_2/CO_2 and N_2/CH_4.

We further analyzed the effects of fillers on membrane performance based on the reported data in the literature (Supporting information Table S3). While some fillers yield membranes whose permeability can be doubled (e.g. H_2 and CO_2); these membranes demonstrate an apparent loss of gas selectivity in some cases, for instance, a drop of H_2/CH_4 selectivity by 26% [29]. In several other cases, incorporation of nanofillers, like COF-300 [32], leads to some increase of gas selectivities; however, the enhancement of gas permeabilities are generally below 41% based on the membranes with a similar loading as this work. In any case, the crystalline PGF-1 based MMMs reside in technologically appealing regions of gas separations with dramatically improved permeability compared with the pristine polymer.

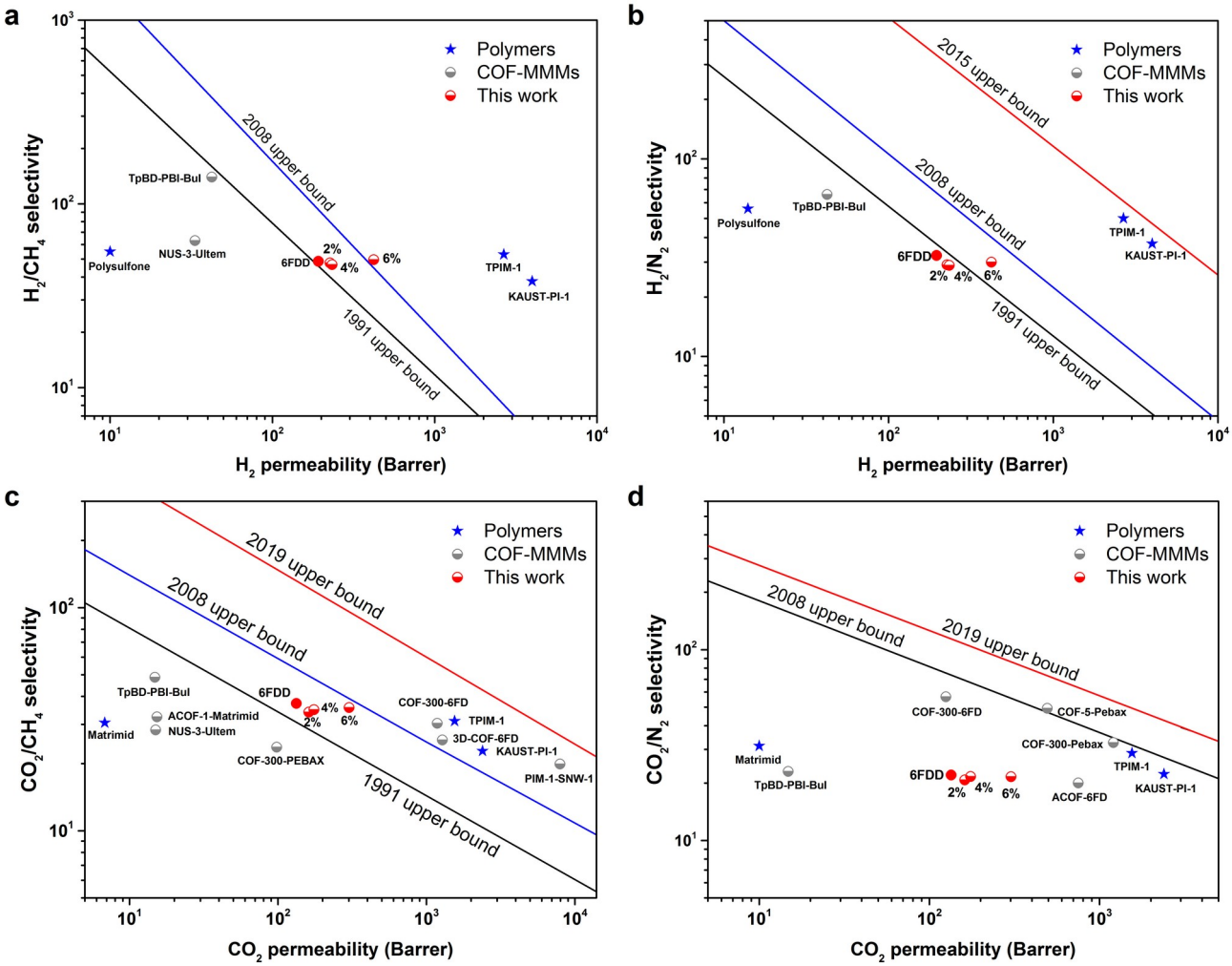

Figure 6. Gas separation performance of PGF-1-6FDD MMMs. (a), H_2/CH_4 (b), H_2/N_2 (c), CO_2/CH_4 (d), CO_2/N_2 separation of PGF-1-6FDD MMMs with PGF-1 loading of 0 wt%, 2 wt%, 4 wt%, and 6 wt%, compared with literature (Supporting Information Table S2). Membrane performance in this work was calculated by averaging at least two separate membrane samples. Membranes were tested at 3 bar, 35 °C.

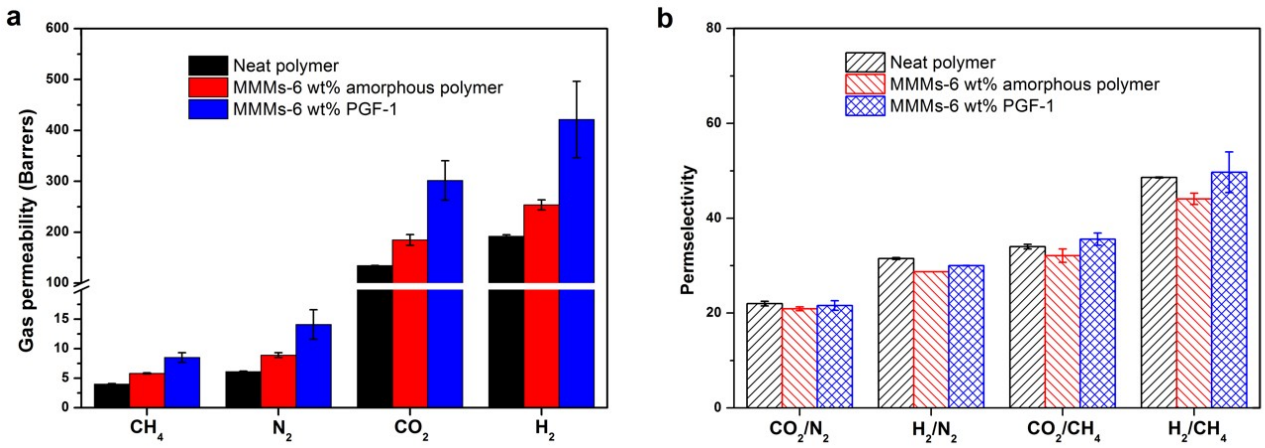

Figure 7. Effect of crystallinity on the separation performance of MMMs. (a) Gas permeability and (b) permselectivity of MMMs made with 6 wt% crystalline PGF-1 or the amorphous counterpart AP-1. The membrane was tested at 3 bar, 35 °C.

3.4. Effects of crystallinity. To further underscore the advantage of using crystalline PGF-1 as a nanofiller for efficient gas separation, the separation performance between PGF-1 and its amorphous analog, AP-1 were compared. It is expected that, when mixing with the 6FDD polymer, the amorphous AP-1 which lacks long-range order and regular pore metrics tends to disrupt the packing of polymer chains and create additional free volume in the interface of AP-1 and polymers [33]. Naturally, this leads to an increase in gas permeability. To validate this hypothesis, we further fabricated AP-1-based MMMs at a loading of 6 wt% to allow rigorous evaluation of the effects of crystallinity on the gas separation performance of MMMs. Gas permeation results were summarized in Figure 7.

As shown in Figure 7, the addition of amorphous AP-1 into 6FDD polymer leads to a slight increase in gas permeability without significantly decreasing the permselectivities. In fact, enhanced permeability of ~40% was observed in AP-1-based MMMs, compared with the pristine polymer. Previous literature has also reported amorphous fillers, such as carbon molecular sieves, can enhance the gas permeability[34]. However, the AP-1-based MMMs demonstrate ~40% lower gas permeability than that of crystalline PGF-1. Note that the AP-1-based MMMs display lower gas selectivity than the crystalline PGF-1 case. The results suggest that owing to disrupting the packing of polymer chains, the amorphous AP-1 can improve gas permeabilities to some degree. However, due to the periodic and uniform pore structures which contribute favorably with more accessible active sites, the crystalline PGF-1 induces more significant enhancement of gas separation performance than its amorphous analog, AP-1.

4. CONCLUSIONS

In summary, for the first time, we successfully demonstrate an effective approach to designing high-performance MMMs using crystalline pyrazine-fused porous graphitic frameworks (PGF-1). By simply using 6 wt% loading of PGF-1, the resulting MMMs exhibit extraordinary gas separation properties, exceeding the current Robeson H_2/CH_4 upper bound. Besides the appealing H_2/CH_4 separation performance, the membranes surpass the prior Robeson upper bounds and approach closely to current Robeson upper bounds for H_2/N_2 and CO_2/CH_4 gas pairs. At the optimal loading of 6 wt%, the MMMs show a H_2 and CO_2 permeability of 421 and 302 Barrers, respectively, with a H_2/CH_4, H_2/N_2, CO_2/CH_4 and CO_2/N_2 selectivity of 49.7, 30.0, 35.6, and 21.6 respectively. The gas permeability is enhanced by over ~120% compared with the pristine polymer without compromising selectivity. Our membranes display 30 times higher permeability compared with a commercially available benchmark polymer, Matrimid®, which has a CO_2 permeability of 10 Barrers[34]. Moreover, the crystalline PGF-1-based MMMs show superior gas separation performance in comparison with that of amorphous polymers, underscoring the importance of establishing long-range order in nanofillers for achieving higher gas separation efficiency. The distinctive properties of membranes based on pyrazine-fused crystalline porous graphitic frameworks enable new approaches to designing highly productive membranes for molecular separations.

ASSOCIATED CONTENT

Supporting Information

The Supporting Information is available free of charge on the ACS Publications website.

Methods of permeability and selectivity calculation, XRD, TGA, FTIR and SEM characterizations ofPGF-1, TGA and FTIR characterizations of membranes, effects of pressures on permeability and selectivity of membranes, H_2/CO_2 and N_2/CH_4 separation

performance, tables showing gas separation performance of this work and membranes reported in literature.

AUTHOR INFORMATION

Corresponding Author

*jianzhang@lbl.gov (J.Z.);yliu@lbl.gov (Y.L.);jjurban@lbl.gov (J.J.U).

Author Contributions

The manuscript was written through the contributions of all authors. All authors have given approval to the final version of the manuscript. ‡These authors contributed equally.

Notes

The authors declare no competing financial interest.

ACKNOWLEDGMENT

Work at the Molecular Foundry was supported by the Office of Science, Office of Basic Energy Sciences, of the U.S. Department of Energy and by the Laboratory Directed Research and Development Program of Lawrence Berkeley National Laboratory under U.S. Department of Energy contract no. DE-AC02-05CH11231. This material is based upon work supported by the Department of Energy under Award Number DE-IA0000018.

REFERENCES

(1) Koros, W. J.; Mahajan, R., Pushing the limits on possibilities for large scale gas separation: which strategies? *J. Membr. Sci.* **2001**, *175,* 181-196.
(2) Koros, W. J.; Zhang, C., Materials for next-generation molecularly selective synthetic membranes. *Nat. Mater.* **2017**, *16,* 289-297.
(3) Jiang, D. E.; Cooper, V. R.; Dai, S., Porous Graphene as the Ultimate Membrane for Gas Separation. *Nano Lett.* **2009**, *9,* 4019-4024.
(4) Wang, L. D.; Boutilier, M. S. H.; Kidambi, P. R.; Jang, D.; Hadjiconstantinou, N. G.; Karnik, R., Fundamental transport mechanisms, fabrication and potential applications of nanoporous atomically thin membranes. *Nat. Nanotechnol* **2017**, *12,* 509-522.
(5) Liu, G.; Jin, W.; Xu, N., Graphene-based membranes. *Chem Soc Rev* **2015**, *44,* 5016-30.
(6) Gadipelli, S.; Guo, Z. X., Graphene-based materials: Synthesis and gas sorption, storage and separation. *Prog. Mater. Sci.* **2015**, *69,* 1-60.
(7) Kim, H. W.; Yoon, H. W.; Yoon, S. M.; Yoo, B. M.; Ahn, B. K.; Cho, Y. H.; Shin, H. J.; Yang, H.; Paik, U.; Kwon, S.; Choi, J. Y.; Park, H. B., Selective Gas Transport Through Few-Layered Graphene and Graphene Oxide Membranes. *Science* **2013**, *342,* 91-95.
(8) Shen, J.; Liu, G. P.; Huang, K.; Jin, W. Q.; Lee, K. R.; Xu, N. P., Membranes with Fast and Selective Gas-Transport Channels of Laminar Graphene Oxide for Efficient CO2 Capture. *Angew. Chem., Int. Ed.* **2015**, *54,* 578-582.
(9) Li, H.; Song, Z. N.; Zhang, X. J.; Huang, Y.; Li, S. G.; Mao, Y. T.; Ploehn, H. J.; Bao, Y.; Yu, M., Ultrathin, Molecular-Sieving Graphene Oxide Membranes for Selective Hydrogen Separation. *Science* **2013**, *342,* 95-98.
(10) Du, H. L.; Li, J. Y.; Zhang, J.; Su, G.; Li, X. Y.; Zhao, Y. L., Separation of Hydrogen and Nitrogen Gases with Porous Graphene Membrane. *J. Phys. Chem. C* **2011**, *115,* 23261-23266.
(11) Kou, Y.; Xu, Y. H.; Guo, Z. Q.; Jiang, D. L., Supercapacitive Energy Storage and Electric Power Supply Using an Aza-Fused pi-Conjugated Microporous Framework. *Angew. Chem., Int. Ed.* **2011**, *50,* 8753-8757.
(12) Wang, L.; Zheng, X. S.; Chen, L.; Xiong, Y. J.; Xu, H. X., Van der Waals Heterostructures Comprised of Ultrathin Polymer Nanosheets for Efficient Z-Scheme Overall Water Splitting. *Angew. Chem., Int. Ed.* **2018**, *57,* 3454-3458.
(13) Marco, A. B.; Cortizo-Lacalle, D.; Perez-Miqueo, I.; Valenti, G.; Boni, A.; Plas, J.; Strutynski, K.; De Feyter, S.; Paolucci, F.; Montes, M.; Khlobystov, A. N.; Melle-Franco, M.; Mateo-Alonso, A., Twisted Aromatic Frameworks: Readily Exfoliable and Solution-Processable Two-Dimensional Conjugated Microporous Polymers. *Angew. Chem., Int. Ed.* **2017**, *56,* 6946-6951.
(14) Lin, L. C.; Choi, J. W.; Grossman, J. C., Two-dimensional covalent triazine framework as an ultrathin-film nanoporous membrane for desalination. *Chem. Commun.* **2015**, *51,* 14921-14924.
(15) Li, X.; Wang, H.; Chen, H.; Zheng, Q.; Zhang, Q.; Mao, H.; Liu, Y.; Cai, S.; Sun, B.; Dun, C.; Gordon, M. P.; Zheng, H.; Reimer, J. A.; Urban, J. J.; Ciston, J.; Tan, T.; Chan, E. M.; Jian Zhang, Y. L., Dynamic Covalent Synthesis of Crystalline Porous Graphitic Frameworks. *Chem* **2020**, 1-12.
(16) Rangnekar, N.; Mittal, N.; Elyassi, B.; Caro, J.; Tsapatsis, M., Zeolite membranes - a review and comparison with MOFs. *Chem. Soc. Rev.* **2015**, *44,* 7128-7154.
(17) Peng, Y.; Li, Y. S.; Ban, Y. J.; Jin, H.; Jiao, W. M.; Liu, X. L.; Yang, W. S., Metal-organic framework nanosheets as building blocks for molecular sieving membranes. *Science* **2014**, *346,* 1356-1359.
(18) Qiu, S. L.; Xue, M.; Zhu, G. S., Metal-organic framework membranes: from synthesis to separation application. *Chem. Soc. Rev.* **2014**, *43,* 6116-6140.
(19) Bachman, J. E.; Smith, Z. P.; Li, T.; Xu, T.; Long, J. R., Enhanced ethylene separation and plasticization resistance in polymer membranes incorporating metal-organic framework nanocrystals. *Nat. Mater.* **2016**, *15,* 845-851.
(20) Chung, T.-S.; Jiang, L. Y.; Li, Y.; Kulprathipanja, S., Mixed matrix membranes (MMMs) comprising organic polymers with dispersed inorganic fillers for gas separation. *Prog. Polym. Sci.* **2007**, *32,* 483-507.
(21) Dong, G.; Li, H.; Chen, V., Challenges and opportunities for mixed-matrix membranes for gas separation. *J. Mater. Chem. A* **2013**, *1,* 4610-4630.
(22) Seoane, B.; Coronas, J.; Gascon, I.; Etxeberria Benavides, M.; Karvan, O.; Caro, J.; Kapteijn, F.; Gascon, J., Metal-organic framework based mixed

matrix membranes: a solution for highly efficient CO2 capture? *Chem Soc Rev* **2015**, *44,* 2421-54.
(23) Cheng, Y. D.; Wang, Z. H.; Zhao, D., Mixed Matrix Membranes for Natural Gas Upgrading: Current Status and Opportunities. *Ind. Eng. Chem. Res.* **2018**, *57,* 4139-4169.
(24) Zhang, C.; Zhang, K.; Xu, L. R.; Labreche, Y.; Kraftschik, B.; Koros, W. J., Highly scalable ZIF-based mixed-matrix hollow fiber membranes for advanced hydrocarbon separations. *Aiche J.* **2014**, *60,* 2625-2635.
(25) Robeson, L. M., The upper bound revisited. *J. Membr. Sci.* **2008**, *320,* 390-400.
(26) Ma, C. H.; Urban, J. J., Hydrogen-Bonded Polyimide/Metal-Organic Framework Hybrid Membranes for Ultrafast Separations of Multiple Gas Pairs. *Adv. Funct. Mater.* **2019**, *29*.
(27) Wu, X. Y.; Tian, Z. Z.; Wang, S. F.; Peng, D. D.; Yang, L. X.; Wu, Y. Z.; Xin, Q. P.; Wu, H.; Jiang, Z. Y., Mixed matrix membranes comprising polymers of intrinsic microporosity and covalent organic framework for gas separation. *J. Membr. Sci.* **2017**, *528,* 273-283.
(28) Duan, K.; Wang, J.; Zhang, Y. T.; Liu, J. D., Covalent organic frameworks (COFs) functionalized mixed matrix membrane for effective CO2/N2 separation. *J. Membr. Sci.* **2019**, *572,* 588-595.
(29) Kang, Z. X.; Peng, Y. W.; Qian, Y. H.; Yuan, D. Q.; Addicoat, M. A.; Heine, T.; Hu, Z. G.; Tee, L.; Guo, Z. G.; Zhao, D., Mixed Matrix Membranes (MMMs) Comprising Exfoliated 2D Covalent Organic Frameworks (COFs) for Efficient CO2 Separation. *Chem. Mater.* **2016**, *28,* 1277-1285.
(30) Li, Y.; Chung, T.-S.; Cao, C.; Kulprathipanja, S., The effects of polymer chain rigidification, zeolite pore size and pore blockage on polyethersulfone (PES)-zeolite A mixed matrix membranes. *J. Membr. Sci.* **2005**, *260,* 45-55.
(31) Comesana-Gandara, B.; Chen, J.; Bezzu, C. G.; Carta, M.; Rose, I.; Ferrari, M. C.; Esposito, E.; Fuoco, A.; Jansen, J. C.; McKeown, N. B., Redefining the Robeson upper bounds for CO2/CH4 and CO2/N2 separations using a series of ultrapermeable benzotriptycene-based polymers of intrinsic microporosity. *Energy Environ. Sci.* **2019**, *12,* 2733-2740.
(32) Cheng, Y. D.; Zhai, L. Z.; Ying, Y. P.; Wang, Y. X.; Liu, G. L.; Dong, J. Q.; Ng, D. Z. L.; Khan, S. A.; Zhao, D., Highly efficient CO2 capture by mixed matrix membranes containing three-dimensional covalent organic framework fillers. *J. Mater. Chem. A* **2019**, *7,* 4549-4560.
(33) Ferrari, M. C.; Galizia, M.; De Angelis, M. G.; Sarti, G. C., Gas and Vapor Transport in Mixed Matrix Membranes Based on Amorphous Teflon AF1600 and AF2400 and Fumed Silica. *Ind. Eng. Chem. Res.* **2010**, *49,* 11920-11935.
(34) Vu, D. Q.; Koros, W. J.; Miller, S. J., Effect of condensable impurity in CO2/CH4 gas feeds on performance of mixed matrix membranes using carbon molecular sieves. *J. Membr. Sci.* **2003**, *221,* 233-239.

Insert Table of Contents artwork here

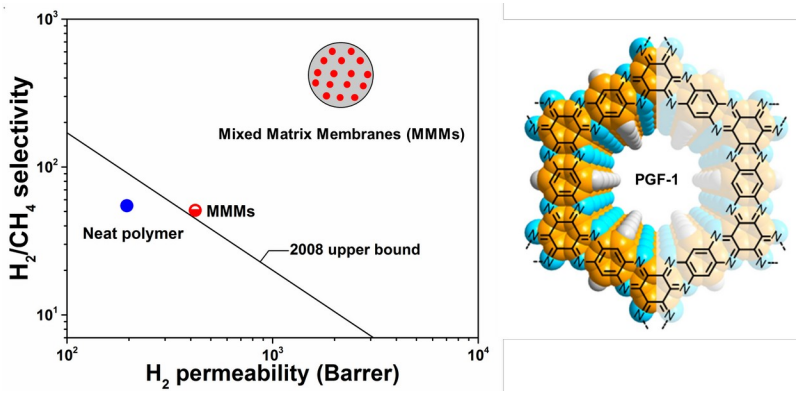

ToC figure

ToC text:

Crystalline pyrazine-fused Porous Graphitic Frameworks (PGFs)/polymer mixed matrix membranes (MMMs) are promising for energy-efficient gas separations such as hydrogen regeneration. Owing to the periodic structures and nitrogen-rich micropores of PGF-1, the MMMs fabricated with a loading as low as 6 wt% of PGF-1 demonstrate gas separation properties surpassing the current Robeson permeability-selectivity upper bound for H_2/CH_4 separation.